

# Early Frontotemporal Dementia Targets Neurons Unique to Apes and Humans

William W. Seeley, MD,<sup>1</sup> Danielle A. Carlin, BA,<sup>1</sup> John M. Allman, PhD,<sup>2</sup> Marcelo N. Macedo, BS,<sup>1</sup> Clarissa Bush, BA,<sup>3</sup> Bruce L. Miller, MD<sup>1</sup> and Stephen J. DeArmond, MD, PhD,<sup>3</sup>

**Objective:** Frontotemporal dementia (FTD) is a neurodegenerative disease that erodes uniquely human aspects of social behavior and emotion. The illness features a characteristic pattern of early injury to anterior cingulate and frontoinsula cortex. These regions, though often considered ancient in phylogeny, are the exclusive homes to the von Economo neuron (VEN), a large bipolar projection neuron found only in great apes and humans. Despite progress toward understanding the genetic and molecular bases of FTD, no class of selectively vulnerable neurons has been identified.

**Methods:** Using unbiased stereology, we quantified anterior cingulate VENs and neighboring Layer 5 neurons in FTD ( $n = 7$ ), Alzheimer's disease ( $n = 5$ ), and age-matched nonneurological control subjects ( $n = 7$ ). Neuronal morphology and immunohistochemical staining patterns provided further information about VEN susceptibility.

**Results:** FTD was associated with early, severe, and selective VEN losses, including a 74% reduction in VENs per section compared with control subjects. VEN dropout was not attributable to general neuronal loss and was seen across FTD pathological subtypes. Surviving VENs were often dysmorphic, with pathological tau protein accumulation in Pick's disease. In contrast, patients with Alzheimer's disease showed normal VEN counts and morphology despite extensive local neurofibrillary pathology.

**Interpretation:** VEN loss links FTD to its signature regional pattern. The findings suggest a new framework for understanding how evolution may have rendered the human brain vulnerable to specific forms of degenerative illness.

Ann Neurol 2006;60:660–667

Primate brain evolution has led to increasing frontal encephalization, hemispheric functional lateralization, and maturational delay. At the level of neuronal morphology, however, little differentiates humans from even our distant mammalian ancestors. Von Economo neurons (VENs) provide a notable exception. These large bipolar projection neurons are a unique feature of great apes and humans.<sup>1</sup> VENs display a simplified dendritic architecture<sup>2</sup> and form small clusters oriented perpendicularly to the brain surface. Paradoxically, VENs are restricted to brain regions often considered ancient in phylogeny, the anterior cingulate cortex (ACC) and frontoinsula (FI).<sup>3,4</sup> Yet, VEN size and clustering increase with phyletic proximity to humans,<sup>1</sup> and VENs are far more abundant in humans than in apes.<sup>5</sup> VENs also mature late in development. In humans, they are identified mainly after birth and reach adult numbers by 4 years of age.<sup>5</sup> Across species, right hemisphere VENs outnumber those on the left, sug-

gesting a role for these cells in social and emotional capacities that distinguish great apes and humans from other primates.

Frontotemporal dementia (FTD), a neurodegenerative condition with a mean onset in the sixth decade of life,<sup>6</sup> provides a potential intersection between brain evolution, VENs, and disease. FTD is as prevalent as Alzheimer's disease (AD) among dementia patients under age 65.<sup>6</sup> Some inherited forms of FTD feature pathological tau-positive neuronal cytoplasmic inclusions associated with mutations in the microtubule-associated protein tau,<sup>7</sup> whereas others have tau-negative, ubiquitin and TDP-43-positive inclusions (FTLD-U) due to mutations in progranulin.<sup>8–10</sup> Yet, most cases of FTD, regardless of the aberrant protein, are sporadic. Across pathological subtypes, early symptoms in behavioral variant FTD reflect a loss of right-lateralized brain capacities that emerge late in childhood and are more robust in great apes and humans than in other primates.<sup>11–13</sup> So-

From the <sup>1</sup>Memory and Aging Center, Department of Neurology and <sup>2</sup>Department of Pathology, University of California, San Francisco, San Francisco, CA; and <sup>3</sup>Division of Biology, California Institute of Technology, Pasadena, CA.

Received Nov 10, 2006, and in revised form Nov 14. Accepted for publication Nov 14, 2006.

B.L.M. and S.J.D. have contributed equally to this work.

This article includes supplementary materials available via the Internet at <http://www.interscience.wiley.com/jpages/0364-5134/suppmat>

Published online Dec 22, 2006 in Wiley InterScience ([www.interscience.wiley.com](http://www.interscience.wiley.com)). DOI: 10.1002/ana.21055

Address correspondence to Dr Seeley, Box 1207, 350 Parnassus Avenue, Suite 706, San Francisco, CA 94143-1207.  
E-mail: [wseeley@memory.ucsf.edu](mailto:wseeley@memory.ucsf.edu)

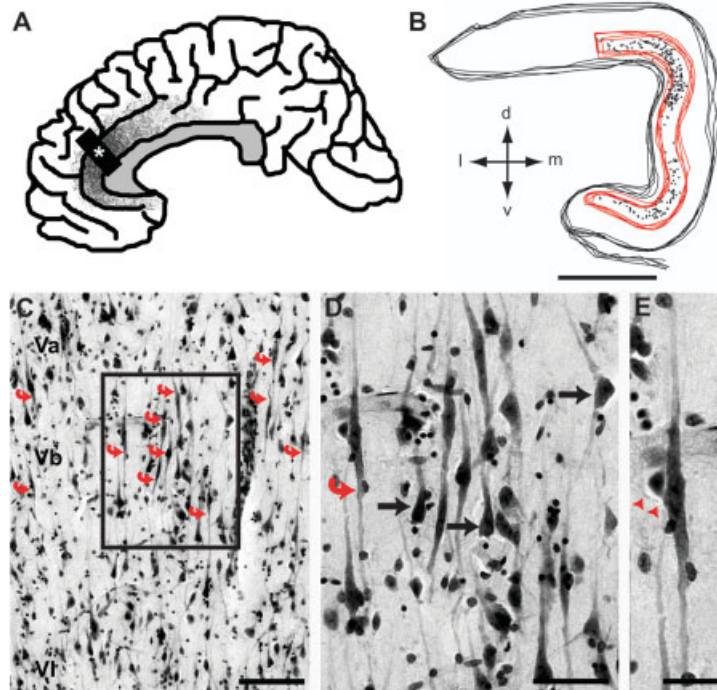


Fig 1. Anterior cingulate sampling site and von Economo neuron (VEN) characteristics in control subjects. (A) VENs are distributed throughout the mid- and anterior cingulate cortex. Dots, drawn schematically based on previous work,<sup>31</sup> highlight the increasing posterior-to-anterior VEN gradient in the normal brain. For this study, tissue blocks were cut from the pregenual anterior cingulate cortex (ACC) (asterisk). (B) ACC VEN distribution in a representative nonneurological control subject. Overlaid contours of the ACC (outer) and Layer 5 (red, inner) were manually traced on 5 to 10 sections per subject. Dots represent VENs, which are concentrated in the crowns of the gyrus. (C–E) VENs (curved red arrows in C) are located in Layer 5b and are distinguished from neighboring neurons (e.g. straight black arrows in D) by their large size and bipolar dendritic architecture. VENs form vertically oriented clusters, often adjacent to small arterioles. Box in (C) is magnified in (D). One of six VENs in (D) is highlighted (curved red arrow) and magnified in (E) to show the typical VEN morphology, including a large VEN axon (red arrowheads). Cresyl violet stain. Scale bars = 3mm (B), 100 $\mu$ m (C), 50 $\mu$ m (D), and 25 $\mu$ m (E). Photomicrographs are oriented with the pial surface at the top. *d* = dorsal; *l* = lateral, *m* = medial, *v* = ventral.

cial and emotional self-awareness, moral reasoning, empathy, and “theory of mind” all deteriorate,<sup>14–19</sup> with catastrophic effects on real-life social behavior. FTD deficits are accompanied by early, focal degeneration of the ACC and FI, often more severe in the nondominant hemisphere.<sup>20–24</sup> The factors that determine this characteristic regional vulnerability pattern remain unknown. Furthermore, because the ACC and FI are classified as paralimbic cortices and are relatively well developed in distant mammals, it is surprising that FTD first affects recently evolved brain functions. Early, selective damage to VENs, however, would resolve this apparent contradiction and help to explain why FTD begins with ACC and FI degeneration.

To determine whether FTD is associated with selective and disease-specific VEN losses, we undertook a quantitative neuroanatomic study of the pregenual ACC (Fig 1) in FTD, AD, and nonneurological control (NNC) subjects.

## Subjects and Methods

### Subjects, Specimens, and Neuropathological Assessment

Archival brain tissues were contributed by the Institute for Brain Aging and Dementia and the University of California, Irvine (UCI) Alzheimer’s Disease Research Center Tissue Resources. Seven NNCs, seven patients with FTD, and five patients with AD were studied. Demographic and autopsy-related variables are shown in Supplementary Table 1. NNC and AD groups were matched to the FTD group for age (one-way analysis of variance [ANOVA],  $F = 0.912$ ;  $p = 0.422$ , not significant) and sex (Pearson’s  $\chi^2 = 0.434$ ;  $p = 0.805$ , not significant). NNC subjects had no known neurological or psychiatric illness and no major structural pathology identified at autopsy. Although most FTD clinical information was recorded before publication of modern FTD research criteria,<sup>25</sup> symptoms described were typical of the FTD spectrum. All FTD subjects had prominent changes in social behavior and emotion, variably combined with deficits in language, memory, or executive function. None had clinical evidence of motor neuron disease or underwent electro-

myography, and none had a first-degree relative with a FTD-related illness. At autopsy, four had Pick's disease, and three had FTL-D-U based on modern immunostaining techniques.<sup>26</sup> Patients with AD, in contrast, showed an array of cognitive symptoms, emphasizing visuospatial, memory, and language impairment, with relative sparing of social functions and behavior. All were clinically diagnosed with probable AD<sup>26</sup> during life and met pathological criteria for high likelihood AD.<sup>27</sup> Comorbid conditions that often accompany AD at autopsy were also found in our subjects: two had Lewy body pathology (diffuse neocortical type in one, transitional limbic in the other), two others had cerebrovascular disease (one had moderate-to-severe atherosclerosis with multiple small acute and remote microinfarcts in gray and white matter; the other had a small, remote intracranial hemorrhage in the left frontal white matter and mild cerebral amyloid angiopathy). No vascular lesion involved the ACC.

Brains were fixed in neutral buffered formalin after a brief postmortem interval (range, 2.5–8 hours) and prepared for evaluation using standard dementia diagnostic procedures.<sup>27</sup> Pathological diagnoses were rendered at the source institution. At both UCI and UCSF, tissue blocks were sampled widely in dementia-relevant brain regions and stained with hematoxylin and eosin and modified Bielschowsky silver stains for initial review. Additional selected sections were stained as indicated for amyloid  $\beta$  peptide,  $\alpha$ -synuclein, hyperphosphorylated tau, and ubiquitin. The study was approved by the UCSF Committee on Human Research.

#### *Disease Stage Assessment*

For each patient with FTD, anatomic disease stage was assessed following a previously validated FTD rating scale (stages 0–4: 0 = normal and 4 = most severe).<sup>23</sup> Photographs of coronal whole-brain 2- to 3cm slabs at the level of the temporal pole and lateral geniculate nucleus were examined by a neuropathologist (S.J.D.) blinded to all quantitative, clinical, and histopathological data. For three patients, only the anterior staging slab remained. Ratings indicated that a range of FTD disease stages was represented, including several patients with borderline or mild atrophy severity (see Supplementary Table 1). If the anterior and posterior slabs differed in stage, subjects were rated according to the more severely affected slab. Anatomic stage and disease duration were at times discordant, perhaps due to difficulties identifying symptom onset or differing rates of progression across patients; tau-positive FTD is known to progress more slowly than tau-negative FTD.<sup>28</sup> In addition, we calculated the mean Layer 5 cross-sectional area from sections used to generate each subject's neuron counting data. This measure showed only a weak inverse correlation with disease stage (Spearman's  $\rho$ ,  $-0.15$ ;  $p = 0.37$ ), perhaps because it fails to reflect change within an individual, but was used to provide a local index of atrophy severity and to confirm that apparent VEN selectivity was not a mere artifact of Layer 5 contraction. Clinical staging data for FTD subjects were not available. All AD patients required full-time care in the months preceding death and were Braak stage VI pathologically.<sup>29</sup>

#### *Tissue Processing and Region-of-Interest Identification*

Previous studies suggest that VENs are restricted to four brain regions, the ACC and FI of each hemisphere.<sup>4,30,31</sup> Because of tissue availability constraints, we evaluated the region most commonly intact in our subjects, the left ACC. Parts of this region had been dissected in each case for diagnostic purposes, precluding exhaustive ACC sampling. Therefore, we analyzed the pregenual ACC, which was intact in all subjects and provides reliable location for VEN sampling.<sup>1,31</sup> Four- to 5mm-thick blocks were dissected at the level indicated in Figure 1. The anterior surface was cut to intersect the corpus callosum as close as possible to 5mm posterior to the tip of the genu and perpendicular to the callosal and cingulate sulci to ensure that VENs fell maximally within the plane of section. Blocks were cryoprotected in successive 10, 20, and 30% sucrose solutions, frozen with dry ice on a freezing stage, and cut at 50 $\mu$ m on a rotary microtome. Resulting sections, numbering 50 to 80 per subject, were Nissl-stained with cresyl violet at an interval of every fifth section and coverslipped. After drying, sections had a minimum thickness of 22 $\mu$ m.

ACC tracings were performed, using Stereo Investigator software (MicroBrightField, Burlington, VT), by a single examiner (W.W.S.) at a microscope-computer interface attached to a motorized stage. First, the outline of the ACC was traced at low power (10 $\times$  magnification) beginning at the lateral recess of the callosal sulcus and ending at a line drawn directly from the recess of the cingulate sulcus to the white matter (see Fig 1). Next, Layer 5 was outlined at higher magnification (40 $\times$  and 100 $\times$ ), based on cell morphological details.<sup>32</sup> We chose Layer 5 as our region of interest (ROI) for neuron counting because VENs are located primarily in Layer 5b.<sup>31</sup> Although VENs can at times be found in Layer 6, we excluded this layer to avoid smaller, spindle-shaped cells or "fusiform" neurons found there more commonly.<sup>1</sup> Pilot data indicated that VENs were scarce in FTD. Therefore, securing reliable estimates required extensive counting within regions of maximum VEN density. For this reason, our Layer 5 ROI encompassed primarily areas 24a and 24b, which feature a much greater VEN density than area 24c.<sup>31</sup> Because the transition from 24b to 24c was at times difficult to discern in patients, we chose an anatomic boundary, ending the superior portion of the Layer 5 ROI at the point where the outer ACC curvature flattened (see Fig 1).<sup>32</sup>

#### *Neuron Quantification*

VENs are thought to make up 1 to 2% of the Layer 5 neurons in ACC.<sup>31</sup> To assess VEN susceptibility, we estimated pregenual ACC VEN and Layer 5 neighboring neuron (NN) populations within the same ROI to afford a ratiometric analysis. This approach has two main advantages. First, tissue atrophy can increase cell density within an ROI, leading to overestimated neuronal integrity when the entire anatomic structure of interest cannot be evaluated. Cell ratios control for this source of error, because cell density increases as a function of ROI contraction, which applies uniformly to each cell type contained within the ROI. Second, the VEN/NN ratio provides an indicator of relative VEN loss, controlled within subjects for overall Layer 5 neuronal loss.

To implement this modified stereological approach, we counted on every fifth section from an arbitrary starting point, the first full-face section from each subject's tissue block. Pilot data indicated that, in control subjects, roughly five sections were needed to achieve reasonable coefficients of error ( $\leq 0.1$ , Schmitz–Hof equation<sup>33</sup>) for the VENs. Therefore, we counted VENs and NNs in no less than five sections per subject, adding sections as needed to achieve a coefficient of error  $\leq 0.1$ . Because VEN counts in FTD patients were often so low, the coefficient of error after 10 sections was accepted if it remained greater than 0.1.

VENs and NNs were counted within the same Layer 5 ROI on separate runs of the optical fractionator.<sup>34</sup> Sampling grid dimensions were set to achieve roughly 200 VEN and 15 NN sampling sites per section. Runs were performed using 400 $\times$  magnification, a 200  $\times$  140 $\mu$ m counting frame, and an 18 $\mu$ m dissector height with 2 $\mu$ m guard zones at top and bottom. Neuron classification was based on morphology. VEN inclusion rules followed published guidelines,<sup>1</sup> requiring the cell to have a visible nucleolus and only two large dendrites oriented at or near 180 degrees from each other, with a basal dendrite as large, or nearly as large, as the apical dendrite. Layer 5 NNs were required to have a visible nucleolus and dendrites to exclude other cells, such as activated glia, that proliferate in disease. A single-point rule (nucleolus) ensured unbiased counting within the counting frame. Tissue atrophy can lead to denser packing of cells in patients. Although this confound should impact VEN and NN density equally, we considered whether VENs would be more difficult to identify in patients because of overlying glia or other neurons. To track VEN determinability, we designated a category for VEN-like cells not counted because of overlying cells that obscured VEN morphological inclusion criteria. The mean number of obscured VEN-like cells per section was similar across groups, slightly higher in NNC and AD than in FTD. Therefore, this potential confound would only have limited our ability to detect a selective VEN reduction in FTD.

Subjects from each diagnostic group were evenly distributed between two raters (D.A.C. and M.N.M.) who had completed a systematic training program. Once the experiment began, if a rater was uncertain about a cell's classification, this cell was marked for later review with the other rater. Though used sparingly, this method promoted consistency and periodic consensus building. The experiment began as a study of FTD and control subjects. FTD-related cellular changes can be appreciated on Nissl stains; therefore, raters could not be realistically blinded to whether a section was from a patient or control subject. After two control and three FTD subjects had been counted, newly available AD subjects were added. At this point, raters were formally blinded to information regarding diagnostic category. Raters were blinded to FTD anatomic stage and histopathological subtype throughout.

Interrater reliability was assessed by having each rater (independently) count every 15th section assessed by the other rater. For intrarater reliability, raters recounted their own N minus 15th section after every 15 sections, where N = total sections counted by that rater throughout the experiment. For interrater reliability, VEN counts from the six sections showed an intraclass correlation coefficient (ICC) of 0.998

(95% confidence interval [CI], 0.993–1.000), and NN counts showed an ICC of 0.987 (95% CI, 0.906–0.998). ICCs computed for intrarater reliability were high and similar for each rater. Combining data from the two raters to yield six sections, the intrarater ICC for VENs was 1.000 (95% CI, 0.987–1.000). For NNs, the ICC was 0.993 (95% CI, 0.949–0.999).

### *Immunohistochemistry*

The archival tissues used for neuron counting were largely inappropriate for immunohistochemical analysis. Therefore, paraffin-embedded 8 $\mu$ m-thick ACC sections from banked UCSF Pick's and FTL-D-U specimens (not included in the study) were examined for Bielschowsky silver, hyperphosphorylated tau (CP-13 antibody, gift of Peter Davies), and ubiquitin (polyclonal antibody; Dako North America, Carpinteria, CA) staining patterns. In addition, recently processed specimens from included AD subjects were reviewed for silver and tau staining characteristics.

### *Statistical Analyses*

Primary analyses examined the effect of diagnostic group on VEN/section, NN/section, and VEN/10<sup>4</sup> NN counts. For these, we used one-way ANOVA and post hoc testing for pairwise group differences using Tukey's multiple-comparison method ( $\alpha = 0.05$ , two-tailed). Quantile-quantile plots indicated that our measures were normally distributed within each diagnostic group, consistent with the assumptions of ANOVA. Supportive analyses assessed group differences in age and ACC/Layer 5 area, also using ANOVA with post hoc Tukey tests. Group differences in sex were assessed using Pearson's  $\chi^2$  analysis. Correlation between Layer 5 area, our indirect measure of disease stage, and VEN/10<sup>4</sup> NN was assessed using Pearson's correlation analysis ( $\alpha = 0.05$ , two-tailed) of the FTD group only ( $n = 7$ ). All statistical analyses were performed using SPSS 12.0 for Windows software (SPSS, Chicago, IL).

## **Results**

Evidence for severe, selective, and early loss of VENs in FTD is shown in Figure 2 and Supplementary Table 2. Compared with control subjects, patients with FTD showed a striking 74% reduction in VENs per section (see Fig 2A). In contrast, and consistent with previous studies,<sup>35</sup> neighboring Layer 5 neurons showed only a mild reduction that was not statistically significant (see Fig. 2B). We examined the degree of selective VEN loss by calculating the number of VENs per 10,000 NNs (VENs/10<sup>4</sup> NNs) for each subject. The FTD group showed a 69% reduction in VENs/10<sup>4</sup> NNs compared with control subjects (see Fig 2C), indicating that VENs are exquisitely sensitive to the FTD degenerative process. Pick's disease, a tau-positive FTD subtype, and FTL-D-U showed similar VEN dropout. Selective VEN losses were seen even in early-stage FTD and did not correlate with Layer 5 collapse (see Fig 2D). These results suggest that VEN injury provides a

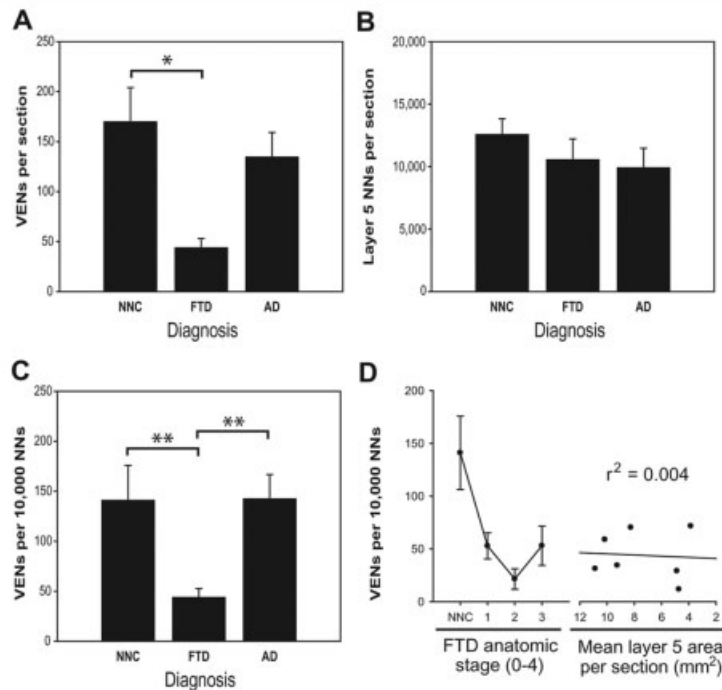


Fig 2. Severe, selective, disease-specific, and early loss of von Economo neurons (VENs) in frontotemporal dementia (FTD). (A) VENs per section were reduced by 74% in FTD compared with nonneurological control subjects (NNC) (\* $p < 0.005$ , Tukey's test after F-test for three-group analysis of variance [ANOVA]). (B) Layer 5 neighboring neurons (NNs), in contrast, showed a mild, statistically nonsignificant reduction in FTD, similar to that seen in Alzheimer's Disease (AD) (see Supplementary Table 2). (C) VEN per 10,000 NN estimates indicated selective VEN depletion in FTD compared with NNC subjects and patients with AD (\*\* $p < 0.05$ , Tukey's tests after F-test for three-group ANOVA). (D) Even mild stages of FTD-related atrophy were accompanied by marked VEN dropout (see Subjects and Methods for staging procedure). Mean Layer 5 area per anterior cingulate cortex (ACC) section, used here as a local marker for disease severity, had no bearing on the VEN/10,000 NN ratio, further suggesting that VEN selectivity occurred across FTD stages. Results are shown as means  $\pm$  standard error of the mean.

key link between FTD and its signature pattern of anterior cingulate and frontoinsular vulnerability.

A previous study reported VEN loss in AD,<sup>31</sup> raising the possibility that VENs are susceptible to multiple forms of neurodegeneration. To address this issue, we studied five patients, age-matched to the FTD group, who were diagnosed with probable AD during life. All had pathological hallmarks of advanced AD. Nonetheless, absolute VEN counts in this group showed only mild, statistically nonsignificant reductions compared with control subjects (see Fig 2A; see Supplementary Table 2). NN loss in AD was similar to that seen in FTD, resulting in a normal VEN/10<sup>4</sup> NN ratio in AD (see Figs 2B, C). In contrast with the previous study,<sup>31</sup> our analysis used unbiased stereological probes, compared younger AD patients with a larger control group, and accounted for NN integrity. Our findings suggest that selective VEN loss is a defining feature of FTD but does not apply to AD. Patients with AD often show intact social graces until late in the illness despite widespread impairments in memory, language, and visuospatial cognition. In direct comparisons, FTD is distinguished from AD by loss of self-awareness,<sup>14</sup> em-

pathy,<sup>19</sup> metacognitive judgment,<sup>14</sup> and behavioral control.<sup>36</sup> Further studies are needed to determine how these functional differences relate to VEN injury.

We found FTD-related changes in surviving VEN size, morphology, and immunohistochemical staining patterns that may provide clues to the mechanisms of VEN susceptibility. Surviving VENs in Pick's disease were often strikingly engorged, in some cases with small, ill-defined, hyperphosphorylated tau deposits littering their proximal dendrites or coalescing within the soma (Figs 3 and 4). Tau supports microtubule stability and axonal transport,<sup>37</sup> and VENs, as large projection neurons,<sup>2,31</sup> may rely heavily on microtubules to deliver organelles, neurofilaments, or peroxisomes to the distal reaches of the cell. Spindle-shaped VEN somata may cope poorly with microtubule cargo backup, resulting in proximal cell distension and accelerated death. In contrast, despite severe VEN losses in FTL-D-U, we have yet to observe significant VEN-associated ubiquitin pathology. FTL-D-U has recently been linked to null mutations in the gene for progranulin, a growth factor associated with cell proliferation and repair.<sup>8,9</sup> Progranulin insufficiency or related

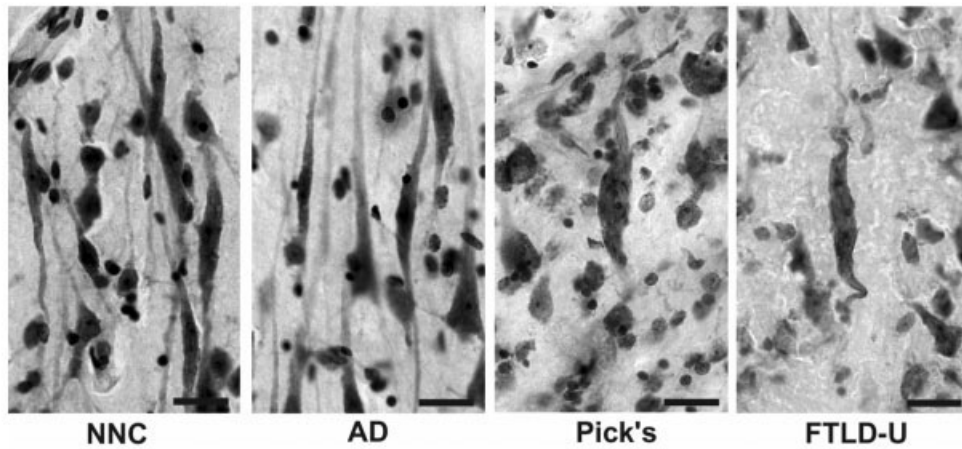


*Fig 3. Von Economo neuron (VEN) swelling and dysmorphism in frontotemporal dementia (FTD). VENs in nonneurological control subjects (NNC) and Alzheimer's disease (AD) patients showed prominent clustering, smooth contours, and slender, tapering somata. In FTD, VENs were often solitary, swollen (especially in Pick's disease), or showed twisting and kinking of proximal dendrites (both Pick's and FTLD-U). Cresyl violet stain. Scale bars = 20 $\mu$ m. Photomicrographs are oriented with the pial surface at the top.*

mechanisms may be particularly deleterious to VENs, a late-developing neuronal population.<sup>5</sup> Twisting and corkscrewing of VEN dendrites were prominent in both FTD subgroups, especially in early stages (see Figs 3 and 4). This feature was not encountered in patients with AD, in whom VENs exhibited normal morphol-

ogy (see Fig 3) and appeared to rarely, if ever, form tangles despite dense neurofibrillary pathology in surrounding cortex (see Fig 4). Because corkscrew morphology can occasionally be seen in control subjects,<sup>4,38</sup> its relevance to cellular function or dysfunction remains uncertain. VEN clustering, a prominent

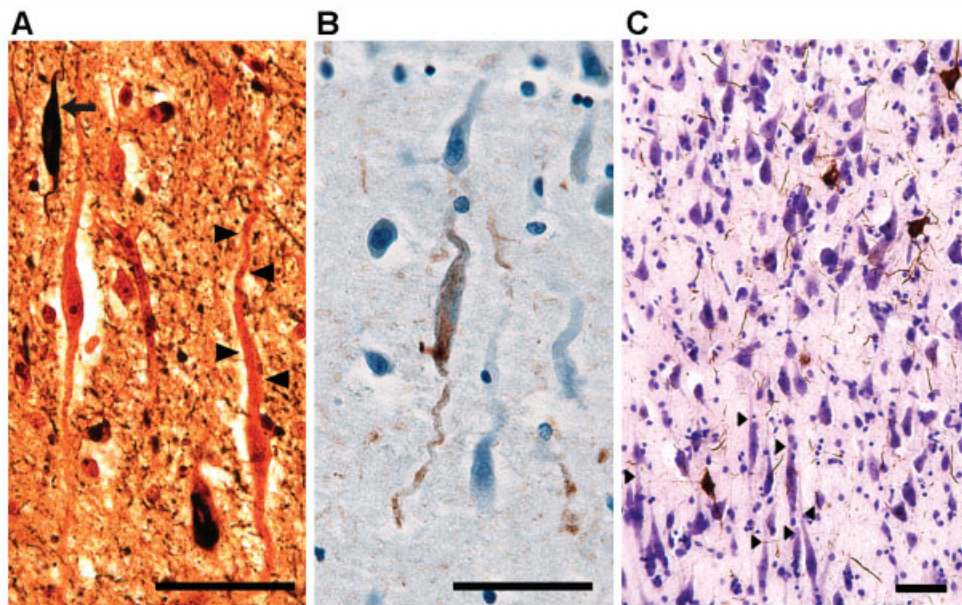


*Fig 4. Frontotemporal dementia (FTD)-associated tau pathology in von Economo neurons (VENs). (A) VENs in Pick's disease, possibly representing distinct stages of degeneration. VENs often showed dense argyrophilic deposits, at times obscuring nearly the entire neuron (arrow). Other VENs showed bloating and undulation of proximal dendrites (arrowheads). A VEN with normal morphology (directly below arrow) provides a comparison. Modified Bielschowsky silver stain. (B) Numerous VENs in Pick's disease showed hyperphosphorylated tau deposition within proximal apical and basal dendrites. CP-13 antibody/hematoxylin counterstain. We have yet to observe classical Pick bodies or ubiquitinated inclusions in VENs. (C) In Alzheimer's disease, normal VEN clusters persisted despite extensive anterior cingulate cortex (ACC) neurofibrillary pathology. Arrowheads point to VEN apical dendrites. CP-13 antibody/cresyl violet counterstain. Scale bars = 50 $\mu$ m. Photomicrographs are oriented with the pial surface at the top.*

feature only in chimpanzees and humans,<sup>1</sup> was rarely seen in FTD but was conspicuous in control subjects and AD. Proximity of VEN clusters to small arterioles (see Fig 1) may reflect high metabolic requirements that exacerbate oxidative VEN injury over the life span.

## Discussion

VENs likely evolved 10 to 15 million years ago,<sup>1</sup> as an ancestor common to great apes and humans took on the neocortical machinery required for complex, agent-oriented social cognition. VEN functions, however, remain unknown, as do the precise behavioral consequences of VEN injury. The ACC and FI represent anatomic transition zones between the paraolfactory-limbic allocortex and the frontotemporal neocortex.<sup>40</sup> As such, they sit poised to convey raw emotional data to top-down modulatory processors. Human VENs, as large, clustered projection neurons with sparse dendritic trees, may sample from a narrow range of inputs before sending a rapid output signal from the ACC and FI to other brain regions.<sup>1,2</sup> Although VEN projection targets are unknown and difficult to study, human functional magnetic resonance imaging connectivity maps reveal that ACC and FI activity levels correlate tightly with each other,<sup>40,41</sup> with peripheral autonomic markers,<sup>42</sup> and with frontotemporal, limbic, and striatal sites<sup>40</sup> that support social cognition and recapitulate the broader FTD anatomic pattern.<sup>22</sup> Our findings support a new concept, that FTD is a disease of brain evolution in which degeneration occurs within an ancient, but recently VEN-enhanced, paralimbic behavioral guidance network.

Further characterization of VENs must move forward while respecting the small group of relevant species. In humans, the VEN somatodendritic compartment appears to express dopamine (D3), serotonin (5HT-1b, 2b), and vasopressin (1a) receptors.<sup>5</sup> VENs may enable these neurochemical systems to process reward, visceral-autonomic, and social-emotional bonding signals in a phylogenetically new way that is derailed in early FTD but spared in AD. In this light, therapies that enhance VEN neurotransmission may help ameliorate FTD symptoms. Basic studies are needed, however, to clarify how VEN biophysical and molecular properties promote VEN degeneration. In FTD, VEN-related dendritic atrophy, synaptic loss, and other markers of neuronal injury may precede frank neuronal dropout and offer an earlier window into disease pathogenesis. The findings of this study should be confirmed in larger series and extended to the frontal insula, where asymmetric VEN loss could relate to behavioral versus language FTD presentations.

Neurodegenerative diseases target specific brain regions and neuronal populations.<sup>43</sup> In FTD research, the finding of ACC and FI atrophy had gone unpaired with a vulnerable cell type. We found that both major

FTD molecular subtypes target a recently evolved neuronal class, VENs, located only in the ACC and FI. Distinctive functions of these unique cells may prove invaluable in health, yet may also expose us to specific forms of developmental<sup>5</sup> or later-life illness. The link forged here between VENs and FTD should spawn further studies of how human brain evolution relates to human brain disease.

## Note added in press

A recent study found VEN-like neurons in the ACC and FI of selected whale species, suggesting convergent evolution in large-brained socially complex mammals [Hof PR & Van Der Gucht E. Structure of the cerebral cortex of the humpback whale, *Megaptera novaeangliae* (Cetacea, Mysticeti, Balaenopteridae). *Anat Rec A Discov Mol Cell Evol Biol* 2006 Nov 27 [Epub ahead of print]].

---

This work was supported by the NIH (National Institute on Aging, K08 AG027086-01, W.W.S.; P01 AG19724-01A1, B.L.M.; P50 AG1657303-75271, S.J.D., B.L.M.), the Larry L. Hillblom Foundation (2005/2T, W.W.S.), Doris Duke Foundation (D.A.C.), and the Gordon and Betty Moore Foundation and David and Lucile Packard Foundation (J.M.A.). The University of California at Irvine Alzheimer's Disease Research Center Neuropathology Core is supported by funding from NIH/NIA P50A916573 and the Institute for Brain Aging and Dementia Tissue Resource is supported by NIH/NIA PO14600538.

We thank E. Head, J. Kaufman, K. Watson, E. Huang, J. Johnson, M. Sattavat, and J. Neuhaus for assistance and E. Roberson and H. Slama for comments on the manuscript. Finally, we thank our patients and their families for participating in dementia research.

---

## References

1. Nimchinsky EA, Gilissen E, Allman JM, et al. A neuronal morphologic type unique to humans and great apes. *Proc Natl Acad Sci U S A* 1999;96:5268–5273.
2. Watson KK, Jones TK, Allman JM. Dendritic architecture of the von Economo neurons. *Neuroscience* 2006;141:1107–1112.
3. Sanides F. Comparative architectonics of neocortex of mammals and their evolutionary interpretation. *Ann NY Acad Sci* 1969; 167:404–423.
4. von Economo C. Eine neue Art Spezialzellen des Lobus cinguli und Lobus insulae. *Z Ges Neurol Psychiatr* 1926;100: 706–712.
5. Allman JM, Watson KK, Tetreault NA, Hakeem AY. Intuition and autism: a possible role for Von Economo neurons. *Trends Cogn Sci* 2005;9:367–373.
6. Ratnavalli E, Brayne C, Dawson K, Hodges JR. The prevalence of frontotemporal dementia. *Neurology* 2002;58:1615–1621.
7. Hutton M, Lendon CL, Rizzu P, et al. Association of missense and 5'-splice-site mutations in tau with the inherited dementia FTDP-17. *Nature* 1998;393:702–705.
8. Baker M, Mackenzie IR, Pickering-Brown SM, et al. Mutations in progranulin cause tau-negative frontotemporal dementia linked to chromosome 17. *Nature* 2006;442:916–919.
9. Cruts M, Gijselinck I, van der Zee J, et al. Null mutations in progranulin cause ubiquitin-positive frontotemporal dementia linked to chromosome 17q21. *Nature* 2006;442:920–924.

10. Neumann M, Sampathu DM, Kwong LK, et al. Ubiquitinated TDP-43 in frontotemporal lobar degeneration and amyotrophic lateral sclerosis. *Science* 2006;314:130–133.
11. Gallup GG Jr. Self-awareness and the emergence of mind in primates. *Am J Primatol* 1982;2:237–248.
12. Lewis M, Sullivan MW, Stanger C, Weiss M. Self development and self-conscious emotions. *Child Dev* 1989;60:146–156.
13. Tomasello M, Carpenter M, Call J, et al. Understanding and sharing intentions: the origins of cultural cognition. *Behav Brain Sci* 2005;28:675–735.
14. Eslinger PJ, Dennis K, Moore P, et al. Metacognitive deficits in frontotemporal dementia. *J Neurol Neurosurg Psychiatry* 2005;76:1630–1635.
15. Miller BL, Seeley WW, Mychack P, et al. Neuroanatomy of the self: evidence from patients with frontotemporal dementia. *Neurology* 2001;57:817–821.
16. Snowden JS, Gibbons ZC, Blackshaw A, et al. Social cognition in frontotemporal dementia and Huntington's disease. *Neuropsychologia* 2003;41:688–701.
17. Lough S, Kipps CM, Treise C, et al. Social reasoning, emotion and empathy in frontotemporal dementia. *Neuropsychologia* 2006;44:950–958.
18. Sturm VE, Rosen HJ, Allison S, et al. Self-conscious emotion deficits in frontotemporal lobar degeneration. *Brain* 2006;129:2508–2516.
19. Rankin KP, Gorno-Tempini ML, Allison SC, et al. Structural anatomy of empathy in neurodegenerative disease. *Brain* 2006;129:2945–2956.
20. Rosen HJ, Gorno-Tempini ML, Goldman WP, et al. Patterns of brain atrophy in frontotemporal dementia and semantic dementia. *Neurology* 2002;58:198–208.
21. Boccardi M, Sabattoli F, Laakso MP, et al. Frontotemporal dementia as a neural system disease. *Neurobiol Aging* 2005;26:37–44.
22. Varrone A, Pappata S, Caraco C, et al. Voxel-based comparison of rCBF SPET images in frontotemporal dementia and Alzheimer's disease highlights the involvement of different cortical networks. *Eur J Nucl Med Mol Imaging* 2002;29:1447–1454.
23. Broe M, Hodges JR, Schofield E, et al. Staging disease severity in pathologically confirmed cases of frontotemporal dementia. *Neurology* 2003;60:1005–1011.
24. Brun A, Gustafson L. Limbic lobe involvement in presenile dementia. *Arch Psychiatr Nervenkr* 1978;226:79–93.
25. Neary D, Snowden JS, Gustafson L, et al. Frontotemporal lobar degeneration: a consensus on clinical diagnostic criteria. *Neurology* 1998;51:1546–1554.
26. McKhann G, Drachman D, Folstein M, et al. Clinical diagnosis of Alzheimer's disease: report of the NINCDS-ADRDA Work Group under the auspices of Department of Health and Human Services Task Force on Alzheimer's Disease. *Neurology* 1984;34:939–944.
27. Consensus recommendations for the postmortem diagnosis of Alzheimer's disease. The National Institute on Aging, and Reagan Institute Working Group on Diagnostic Criteria for the Neuropathological Assessment of Alzheimer's Disease. *Neurobiol Aging* 1997;18:S1–S2.
28. Roberson ED, Hesse JH, Rose KD, et al. Frontotemporal dementia progresses to death faster than Alzheimer disease. *Neurology* 2005;65:719–725.
29. Braak H, Braak E. Neuropathological staging of Alzheimer-related changes. *Acta Neuropathol* 1991;82:239–259.
30. von Economo C, Kosinkas GN. *Die Cytoarchitektonik der Hirnrinde des Erwachsenen Menschen*. Berlin: Springer, 1925.
31. Nimchinsky EA, Vogt BA, Morrison JH, Hof PR. Spindle neurons of the human anterior cingulate cortex. *J Comp Neurol* 1995;355:27–37.
32. Vogt BA, Nimchinsky EA, Vogt LJ, Hof PR. Human cingulate cortex: surface features, flat maps, and cytoarchitecture. *J Comp Neurol* 1995;359:490–506.
33. Schmitz C, Hof PR. Recommendations for straightforward and rigorous methods of counting neurons based on a computer simulation approach. *J Chem Neuroanat* 2000;20:93–114.
34. Gundersen HJ, Bagger P, Bendtsen TF, et al. The new stereological tools: disector, fractionator, nucleator and point sampled intercepts and their use in pathological research and diagnosis. *Apmis* 1988;96:857–881.
35. Kersaitis C, Halliday GM, Kril JJ. Regional and cellular pathology in frontotemporal dementia: relationship to stage of disease in cases with and without Pick bodies. *Acta Neuropathol (Berl)* 2004;108:515–523.
36. Bathgate D, Snowden JS, Varma A, et al. Behaviour in frontotemporal dementia, Alzheimer's disease and vascular dementia. *Acta Neurol Scand* 2001;103:367–378.
37. Trojanowski JQ, Lee VM. Pathological tau: a loss of normal function or a gain in toxicity? *Nat Neurosci* 2005;8:1136–1137.
38. Allman JM, Hakeem A, Erwin JM, et al. The anterior cingulate cortex. The evolution of an interface between emotion and cognition. *Ann NY Acad Sci* 2001;935:107–117.
39. Mesulam MM. From sensation to cognition. *Brain* 1998;121(pt 6):1013–1052.
40. Seeley WW, Menon V, Schatzberg AF, et al. Human resting-state cortical-subcortical networks for salience processing and executive control. *Neuroimage* 2006;31(S1):S20.
41. Beckmann CF, DeLuca M, Devlin JT, Smith SM. Investigations into resting-state connectivity using independent component analysis. *Philos Trans R Soc Lond B Biol Sci* 2005;360:1001–1013.
42. Critchley HD. Neural mechanisms of autonomic, affective, and cognitive integration. *J Comp Neurol* 2005;493:154–166.
43. Hyman BT, Damasio AR, Van Hoesen GW, Barnes CL. Alzheimer's disease: cell-specific pathology isolates the hippocampal formation. *Science* 1984;298:83–95.